PERSPECTIVES FOR A WIND ASSISTED SHIP PROPULSION

(DOI No: 10.3940/rina.ijme.2018.a1.439)

M Bentin, S Kotzur, M Schlaak, D Zastrau, University of Applied Sciences Emden-Leer (HSEL), Germany and
D Freye, University of Applied Sciences Osnabrück, Germany

SUMMARY

For three different wind propulsion technologies, the energy saving potential of sea going cargo vessels are discussed: a kite, a Flettner rotor and a Dynarig-sail. The energy saving potential can be increased significantly if the route can be optimized when using a wind assisted ship propulsion. The increase of travelling time due to a route adoption is within the frame of the commonly accepted uncertainty in supply chains and can be limited or adjusted in the route optimization software as a parameter. The calculated saving potential depends on several parameters: the considered wind propulsion system, the route, the kind of ship (bulker, multipurpose carrier, tanker), as well as the ship speed and the weather. The cost-effectiveness of the installation of a wind propulsion system strongly depends on the fuel price, the ship speed and the international policy concerning the ship emissions.

1. INTRODUCTION

The most important cost factor in ship transportation is the fuel price, 40 % to 60 % , depending on the global fuel price situation (bunkerindex, 2016; Bunker Fuel Prices).There are several approaches to minimize the fuel consumption of ships as slow steaming, operating the engines in the most effective range, ship design, hybrid technologies for ship propulsion. One option for a hybrid system is the Wind Assisted Ship Propulsion WASP using wind for a part of the propulsion systems, which means that the engine power can be reduced using a Wind Propulsion System WPS, when the weather conditions are suitable. This kind of hybrid propulsion is not new, but in the past it came up from another technological direction: In the beginning of the 19th century the steam engine started to replace the sails on seagoing ships. For instance, in 1854 /56 the "Great Eastern" used steam engines to support the sail propulsion. In the beginning of the 20th century the steam engines and the last sails were replaced by fuel driven motors, due to the easy availability of this fuel and the enormous saving potential by ship design (no rags on deck, smaller machineries) and personnel reduction. The perspectives for the use of a WASP is guided by the strong pressure for cost reduction, by the environmental impact from ship emissions (CO_2, SO_2, NO_x, particles ...), and by the long-term view on the availability of oil.

So the use of wind propulsion systems as a WASP comes up under new perspectives (Otto, 1992; Schenzle and Hollenbach, 2010; Schenzle, 2016; Traut et al., 2014). However, the transport capacity, the cargo handling and the amount of personnel on the ship should not be negatively influenced by the use of a WPS.

The energy saving by a WPS depends on the weather conditions along the ship's route: wind produces propulsion energy by the WPS, but it also produces waves, which consume propulsion energy, when the ship is steaming against wind, and waves. When using WASP it is important to adopt the route for an optimal use of the wind energy. However, this route optimization shall not lead to an essentially longer travelling time, which might decrease the profitability of the cargo transport. So it cannot lead to the ancient ship routes for sailing ships. Based on these conditions appropriate WPS and a suitable route optimization are discussed in this paper. The uncertainty in weather prediction leads to an uncertainty in the route optimization for the saved energy and the estimated time of arrival (ETA) and can be taken into account (Zastrau, 2016).

2. CONCEPT

For a realistic discussion of the future of WASP systems modern WPS, suitable ship types and typical ship routes are selected.

2.1 WIND PROPULSION SYSTEMS (WPS)

The future use of WPS for WASP is under discussion since many years (Otto, 1992; Schenzle, 2010; Dykstra Naval Architects, 2013; Allenström, 2012). Here the following criteria for the use of a WPS in a WASP are considered:

- New interesting features for WPS (with high efficiency, low impact on the ship performance)
- State of the technology (already realized for instance in pilot installations)
- Suitability for installation on existing cargo ship types
- The influence on ship performance (loading, unloading, handling during the steaming period)
- No additional crew necessary

As a result, the following WPS were chosen (Figure 1):

- a kite
- Flettner-rotors
- a Dynarig

Figure 1: Different wind propulsion systems (WPS) used for wind assisted ship propulsion (WASP): a kite (top-left), Flettner rotors (bottom-left), soft furling square sails (Dynarig sails on the Maltese Falcon, bottom-right), solid foldable square sails with a similar function as the Dynarig (Shin Aitoku Maru, top-right).

2.2 SHIPS

The following criteria are considered for suitable ship types:

- cargo ships with a common speed of about 13 – 15 kn. Ships with a higher speed as e.g. 20 kn or more (Container ships, Ferries, Passenger Ships, …) can only use a small part of the wind spectra (wind speeds > 6 Bft) for WASP.
- The ship types should be suitable for the installation of WPS without changing the function of loading and unloading of a cargo or the capacity of the ship.
- The ship types considered should realize an essential part of the international cargo transport.
- The transport time of the ships should have a certain tolerance, which is given for the tramp shipping (not valid for container ships, ferries, ..)

For the simulation the following ships are chosen as typical examples of the three chosen ship types:

- a multi-purpose carrier (MPC): 17 500 DWT, length pp: 133m, width: 22.8 m
- a bulker: 37 600 DWT, length pp: 183 m, width: 28.5 m
- a tanker: 114 000 DWT, length pp: 240 m, width: 44 m

2.3 ROUTES

The efficiency of a WASP system depends on the weather conditions on a route. There are typical differences in the weather situation on different areas of the oceans: the areas near the poles have higher average wind speeds than the areas near the equator (not counting special situations like hurricanes). The following criteria are considered to select appropriate shipping routes:

- The distance (long and short distances)
- The weather conditions (dominant high or low wind speeds)
- Routes used for an essential part of the global good transport

Therefore, the following routes are chosen:

- Germany – North America: Wilhelmshaven – Baltimore, a medium range route in a strong and turbulent wind field area with a dominant wind direction (west-east)
- Germany - South-America: Emden - Nueva Palmira, a long-range route with rather stable weather situations with normally low wind speeds.
- Germany – Norway: Wilhelmshaven – Bergen, a short-range route with turbulent weather conditions in both directions.

3. WIND PROPULSION SYSTEM

3.1 SIMULATION CONCEPT

The propulsion force of the discussed WPS is modelled based on available literature data. The energy saving potential is simulated using models for the ship resistance and the ship propulsion, taking into account the additional resistances due to waves and wind for the actual weather situation (Bentin *et al*., 2016). The propulsion force FP of a WPS is given by

$$FP \sim A * FPN(AWS, AWA, C_l, C_d)$$

A characterizes the dimension of a WPS.
C_l, C_d lift and the drag coefficients respectively
AWS apparent wind speed, AWA: apparent wind angle

FPN(AWS, AWA, C_l, C_d) describes the „normalized“ propulsion force of a WPS as function of the direction and the speed of the apparent wind (AWA, AWS) and the WPS characterizing parameters C_l and C_d.

The propulsion force FP of the WPS will provide an effective additional propulsion power P_e(WPS) = FP*Vs at a certain ship speed Vs through water (STW).

The necessary effective propulsion power to overcome the resistance due to the ship speed through calm water (cw) and due to wind and waves is

$$P_e = P_e(cw) + P_e(wind) + P_e(waves) \ .$$

With the WPS and the reduced engine power (for wind assisted hybrid propulsion) P_e(WASP) the effective propulsion has two components

$$P_e = P_e(WASP) + P_e(WPS) \quad or$$
$$P_e(WASP) = P_e - P_e(WPS)$$

The corresponding break power P_B supplied by the engine is

$$P_B(WASP) = \frac{1}{\eta_T} Pe(WASP) = \frac{1}{\eta_T}(P_e(cw) + P_e(wind) + P_e(waves) - P_e(WPS)),$$

With η_T = total efficiency between break power delivered by the engine and the effective propulsion power. The break power is related to the fuel consumption m of the motor via the Specific Fuel Oil consumption SFOC:

$$m = SFOC\ P_B .$$

The reduction of consumption due to P_e(WPS) is

$$\Delta m(WPS) = SFOC\ \frac{1}{\eta_T} P_e(WPS)$$

η_T may change due to the reduced load on the propeller by the WPS. However we use a constant η_T in the simulation, which might be realized by a propeller with an adjustable pitch (see E-Ship1). The contribution due the calm water resistance P_e(cw) is taken from the model test report of the specific ship and those due to wind and waves are simulated according to software / formula available in literature and evaluated by actual ship measurements over 2 years (Schlaak, 2016; Bentin *et al*., 2016).

3.2 KITE

The function and the use of a kite has been described in (Schlaak *et al*., 2009). The model is based on the energy calculation for wind turbines. The wind power

$$P_{wi} = \frac{1}{2} * \rho * V_{wi}^3 * S_{wi}$$

(V_{wi} = wind speed, S_{wi}=effective wind surface, ρ = air density) is related to a "wind force F_{wi}" by

$$P_{wi} = (\boldsymbol{F_{wi}}) * (\boldsymbol{V_{wi}})$$

(bold letters signify vectors). The wind force F_{wi} causes a force on the kite: FP. The efficiency of the energy transfer from the wind field to the kite is considered by ε

$$FP = \frac{1}{2} * \rho * AWS^2 * \varepsilon * S_{wi} * FPN$$

By comparing with experiments, the model is fitted giving

$$FP = 27N \left(\frac{A}{m^2}\right) \left(\frac{\mathrm{AWS}}{m^s}\right)^p FPN \quad \text{with}$$

$$FPN = \left(cos\frac{\alpha}{2}\right)^2 (cos\ \delta)^2 = \left(cos\frac{180° - \mathrm{AWA}}{2}\right)^2 (cos\ \delta)^2$$

FPN normalized propulsion force as function of the direction of the wind, independent of the size of the kite and the wind speed
AWS apparent wind speed
A dimension (surface) of the kite

α = 180°- AWA

δ = 30° elevation angle of rope from ship to kite

p dependent of the speed of the kite: 1- 2

The kite is sailed on a laying 8, the central point is positioned in the direction of half angle between ship course and AWA.

The used weather data refer to 10 m above sea level. Since the kite is sailed well above the ship (e. g. 100 m) the wind speed V_{Wi} (h) in the height h is calculated by

$$V_{Wi}(h) = V_{Wi}(10m) \frac{ln\frac{h/m}{10^{-2}}}{ln10^3}$$

The normalized propulsion force FPN characterizes the behavior of the kite as a function of the apparent wind angle AWA (Figure 4). The propulsion power P_e (WPS) is (V_S = ship speed through water STW)

$$P_e(kite) = FP * V_S$$

And the corresponding reduction of the engine power (brake power)

$$\Delta P_B = \frac{1}{\eta_T} P_e(kite)$$

To drive the kite on the 8 an electrical motor is used, consuming a certain small amount of electrical energy P_{EE}, which reduces the fuel saving by the kite $\Delta m(kite)$ with a specific motor efficiency SFC

$$\Delta m(kite) = SFOC\ \frac{1}{\eta_T}\ P_e\ (\mathrm{kite}) - SFC\ P_{EE}$$

but is considered in the simulation by a reduction of the break power saving by the kite

$$\Delta P_B\ (kite) = \frac{1}{\eta_T}\ P_e(\mathrm{kite}) - \frac{1}{\eta_{EE}} P_{EE}\ (\mathrm{kite})$$

η_{EE} characterizes the efficiency of creating electricity by a fuel burning machine on board.

The final break power for the hybrid system is:

$$P_B(WASP) = P_B(withou\ WPS) - \Delta P_B\ (kite) = \frac{1}{\eta_T}\left(P_e(cw) + P_e(wind) + P_e(waves)\right) - \frac{1}{\eta_T} P_e(kite) + \frac{1}{\eta_{EE}} P_{EE}(\text{kite})$$

3.3 FLETTNER

The Flettner-rotor creates a force perpendicular to the direction of the apparent wind (Magnus effect based on Bernoulli, see e.g. (Seifert, 2012)). This effect depends on the rotation speed of the rotor and the wind speed. The optimal rotation speed depends on the apparent wind angle. Often the relation between wind speed and the peripheral surface speed is in the range of 3 to 4 (Wagner *et al*., 1985; Seifert, 2012).

As a ship propulsion, the Flettner rotor was first installed in 1924 on the "Buckau" (2 Flettner rotors) and in 1926 on the "Barbara" (3 rotors). Both ships were sailing with the Flettner rotors for several years. As the fuel driven ships became more economic WPS systems such as the Flettner were not used anymore. The rising fuel price and the impact of the ship emissions on the environment has brought the Flettner rotor back into discussion. In 2008 the E-ship 1 of ENERCON was constructed with 4 Flettner rotors (see Figure 1).

The propulsion force can be described by

$$FP = \frac{\rho}{2} A_F\ AWS^2\ (C_l \sin\beta - C_d \cos\beta) = \frac{\rho}{2} A_F\ AWS^2\ FPN$$

with

η	density of air
AWS	apparent wind speed
A_F	relevant surface for the rotor = L * D with L = height of rotor, D = diameter of rotor
D_s	diameter of top disc with $D_S \geq 2D$ (to avoid an early break down of the flow structure)
β	angle between ship course and the direction of the apparent wind AWS
C_l, C_d	lift and drag coefficients

For the calculation of the Flettner characteristics $FPN = f(C_l, C_d,$ AWA) the experimentally established dependencies for C_l and C_d are used (Wagner *et al*., 1985)

$$C_l = C_l\left(\frac{u}{AWS}\right) und\ C_d = C_d\left(\frac{u}{AWS}\right)$$

u peripheral speed of the rotor (m/sec)

For the Flettner rotor the C_l and C_d coefficients depend on the relation between peripheral speed of the rotor surface u and AWS: $x = \frac{u}{AWS}$. For x = 4 there is a maximum for C_l, so that for the model the following conditions are set: $x = \frac{u}{AWS} \leq 4$. There is a limit of the rotor speed $n = n_{max}$ due to technical limitations:

$$u \leq u_{max} = \pi D n_{max}$$

The calculated polar based on these C_l, C_d values is shown in Figure 4.

The propulsion power contribution of the Flettner Rotor is

$$P_e(Fl) = FP(Fl)\ V_S$$

It decreases the propulsion energy required by the machine to keep Vs (brake power P_B) by:

$$\Delta P_B(Fl) = \frac{1}{\eta_T} P_e(Fl)$$

Rotation energy of the rotor

The Flettner rotor needs electrical energy for the rotation of the cylinders. This energy is supplied by electrical motors and is mainly needed to overcome the friction due to the rotation. The friction can be described by (Wagner *C. et al*., 1985):

$$F_R = c_R * F_N$$

c_R	friction coefficient, dependent on the kind of the bearing
F_N	weight force of the rotor weight

The power to overcome the friction is

$$P_R = F_R u = F_R\ 2\pi R n = c_R\ m_R\ g\ \pi\ D\ n$$

u	peripheral speed of the rotor surface shell
m_R	$= d\pi DH\rho_M$ (mass of the rotor)
d	thickness of the rotor shell
D	diameter of the rotor,
H	height of the rotor
ρ_M	density of the rotor material
n	revolution speed.

The formula is compared with the value given for the E-Ship 1 (ENERCON, 2013) and fitting the C_R value gives

$$P_R = RFL\ \left(\frac{D}{m}\right)^2 \left(\frac{H}{m}\right)\left(\frac{n}{\frac{1}{min}}\right) kW = P_{EE}$$

with $RFL = \frac{1}{400} = 2{,}5\ 10^{-3}$

The aerodynamic friction is neglected, estimated to be essentially smaller than the mechanical fraction. The effective reduction of the ship propulsion power of the

Flettner rotor has to be reduced by the rotation energy needed, supplied by an electricity generator as P_{EE}

$$\Delta P_B(Fl) = \frac{1}{\eta_T} P_e(Fl) - \frac{1}{\eta_{EE}} P_{EE}(Fl)$$

η_{EE} for the efficiency of creating electricity by fuel burning on board.

The final break power for the wind assisted hybrid system is:

$$\begin{aligned} P_B(WASP) = \; & P_B(without\ WPS) - \Delta P_B\ (Fl) \\ & = \frac{1}{\eta_T}\big(P_e(cw) + Pe(wind) \\ & + P_e(waves)\big) - \frac{1}{\eta_T} P_e(Fl) \\ & + \frac{1}{\eta_{EE}} P_{EE}\ (\mathrm{Fl}) \end{aligned}$$

3.4 DYNARIG

The Dynarig is a development of the square sail into the direction of the Bermuda sail for a more effective wind use for sailing close to the wind. The sail is constructed as a segment circle attached to the yards and uses the Bernoulli effect for ship headings near to the apparent wind direction (Figure 2). The Dynarig was designed by Prölss and researched by Wagner (Prölss, 1970; Wagner, 1966). In 2006 the Dynarig was realized on the "Maltese Falcon ", a 88 m yacht (www.decaboyachtpainting.com; Maltese Falcon, 2016) (Figure 1). A transport ship with the Dynarig ("The Ecoliner") is discussed (Dykstra Naval Architects, 2013).

The apparent wind causes a lift force L and a drag force D at the Dynarig (Figure 2):

$$L = C_l \frac{\rho}{2} A_S\ AWS^2$$
$$D = C_d \frac{\rho}{2} A_S\ AWS^2$$

A_S surface of the sail
C_l, C_d lift and drag coefficients

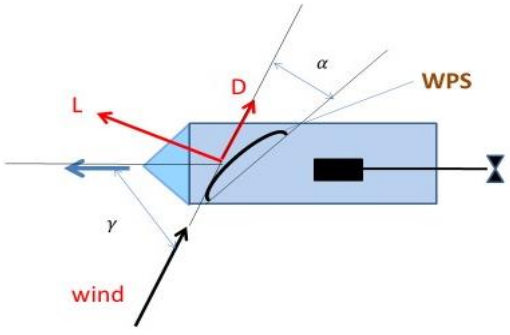

Figure 2: Forces (L, D) and angles at the Dynarig

The propulsion force results in

$$\begin{aligned} FP(DR) &= L\sin\gamma - D\cos\gamma \\ &= \frac{\rho}{2} A_S\ AWS^2\ (C_l\ \sin\gamma - C_d\ \cos\gamma) \\ &= \frac{\rho}{2}\ A_S\ AWS^2\ FPN(DR) \end{aligned}$$

The normalized force FPN is a function of γ, the direction of the apparent wind in relation to the ship course and the position of the sail α in relation of the AWA. C_L and C_d depend on the angle between the direction of the AW to the sail. For the modelling of the function of the sail the C_L and C_d values are taken from Figure 3, based on experimental measurements in the wind tunnel.

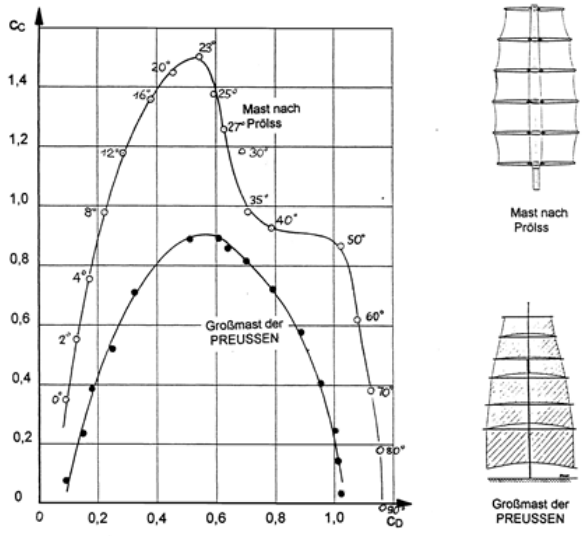

Figure 3: Diagram of C_l (here Cc) and C_d (here C_D)values as function of α , the orientation of the sail to the apparent wind direction AWA form (Wagner, 2000)

$\alpha = 90°$ means pure drag function of the sail. For $\alpha = 23°$ the course close to the wind C_l has a maximum. For the calculation of the polar diagram $FPN = f(\gamma, \alpha)$ (Figure 4) γ is varied and α is choosen for an optimal performance.

The propulsion power of the Dynarig

$$P_e(DR) = F(DR)\ V_S$$

reduces the machine propulsion power by

$$\Delta P_B(DR) = \frac{1}{\eta_T} P_e(DR).$$

The final break power for the hybrid system is:

$$\begin{aligned} P_B(WASP) = \; & P_B(without\ WPS) - \Delta P_B\ (DR) \\ & = \frac{1}{\eta_T}\big(\ P_e(cw) + P_e(wind) \\ & + P_e(waves)\big) - \frac{1}{\eta_T} P_e(DR) \end{aligned}$$

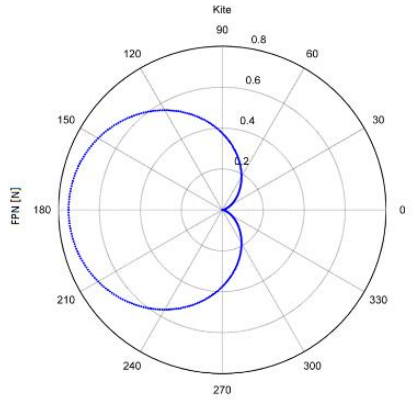

(a)

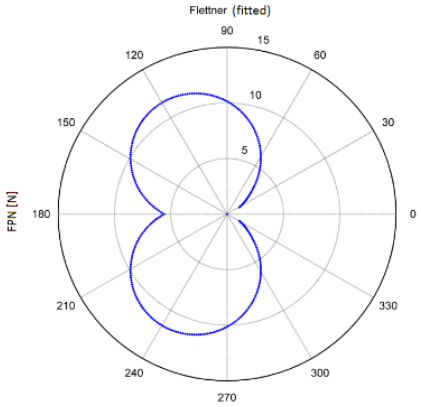

(b)

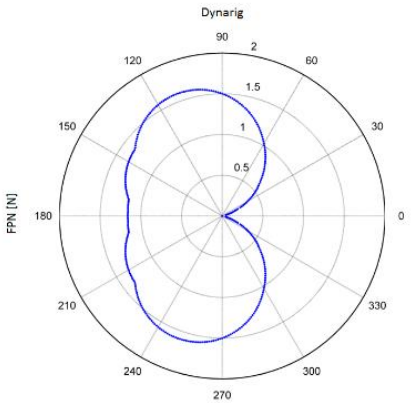

(c)

Figure 4: The normalized propulsion force FPN [N] for the discussed WPS as function of the apparent wind direction AWA. (a) kite: elevation angle δ = 30°; (b) Flettner rotor: values for AWS = 10 m/s, the asymmetry of the polar is due to the C_l and C_d values selected for optimal performance; (c) Dynarig: For stern winds, the positioning of the sail α is not adopted continuously, but only stepwise, a practical approach to avoid resonance effects due to movements of the ship in the sea.

3.5 SPECIFICATIONS OF THE DISCUSSED WPS

While the kite shows high efficiency for stern winds, the Flettner has maximum efficiency for lateral winds, the Dynarig not only shows a high effect for lateral winds (Bermuda sail characteristics) but also a reasonable efficiency for stern winds (Figure 4).

To simulate the energy saving potential of the discussed WPS they have to be dimensioned and positioned on the selected ships. For the dimensions, somewhat realistic values were selected based on the realization of the Flettner rotors on the E-ship 1. The dimensions of the kite and the Dynarig are chosen so that the wind force is about the same for the three systems for lateral winds. Interactions between different units (rotors or masts) on the ship are neglected.

DR: Dynarig
A = 800 m for each mast
H = 30 m: average height of area exposed to wind
N = 3: number of masts

KI: Kite
A = 800 m : area of the kite
H = 150 m: mean sailing height of the kite
δ= 30° elevation angle
P_{EE}=2 kW: energy for the kite motor, positioning and moving the kite
η_{EE} = 0.9 efficiency to produce electricity on board

FL: Flettner
H= 25 m height of the rotors
D = 4 m: diameter of the rotors
DS = 8 m: diameter of the end disc on the rotor:
DS = 2* D for the C_d, C_l values used
H= 30 m: mean height of the wind field used:
n_{max}= 200(1/min) maximal rotation speed
η_{EE} = 0.9: efficiency to produce electricity on board
N=4: number of rotors

4. ROUTE OPTIMIZATION

For an optimal use of the WPS on a route the course of the ship can be adjusted to select the route with the best weather conditions for the WPS. An appropriate route optimization tool (including the influence of wind and waves directly on the ship) has been developed (Bentin *et al*., 2016). Figure 5 shows an example for a shortest route (great circle) and an optimized route. Routes with a travelling time longer than 20% compared to the travelling time on the great circle GC and routes, where the ship encounters bad weather (e.g. waves over 5 m height,) are discarded.

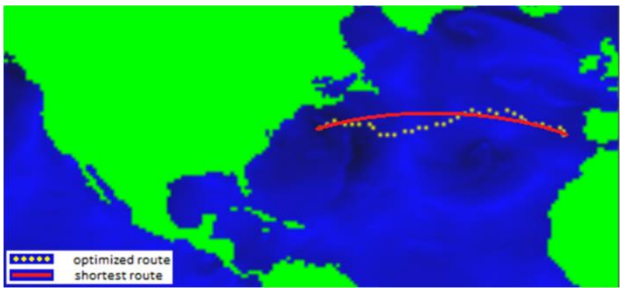

Figure 5: Ship course changed from the great circle GC (red) to an energy optimized route RO (dotted line), when using a WASP (Bentin *et al*., 2016)

5. RESULTS

The energy saving potential depends on the ship, the ship performance (ship type, ship speed, ship course), the technology and size of the WPS and the weather conditions. To demonstrate the saving potential by the discussed WPS the energy consumption of the 3 discussed ship types and the three discussed WPS have been simulated on the three selected routes (chapter 2).

The energy saving is simulated for courses on the great circles (GC) and for optimized routes (RO). The results are presented for a given fixed ship speed of 13 kn (STW). Figure 6 shows the simulation results for a multi-purpose carrier (MPC) on the route from Baltimore (USA) to Wilhelmshaven (Germany). Mean values and the distribution of the simulated values are calculated for one journey per week with historical weather data from the year 2008. As weather data, the historical analysis data of the "Deutscher Wetterdienst" DWD were taken along the route at the specific time, the ship being at that position of the route.

The results for the following scenarios are presented:

(a) Energy saving by RO without WPS ("Sea-margin")

The additional energy needed due to wind and waves (sea margin) is shown in Table 1 for the 3 selected routes. With the route optimization, the sea margin can be reduced significantly on routes with strong winds (North Atlantic).

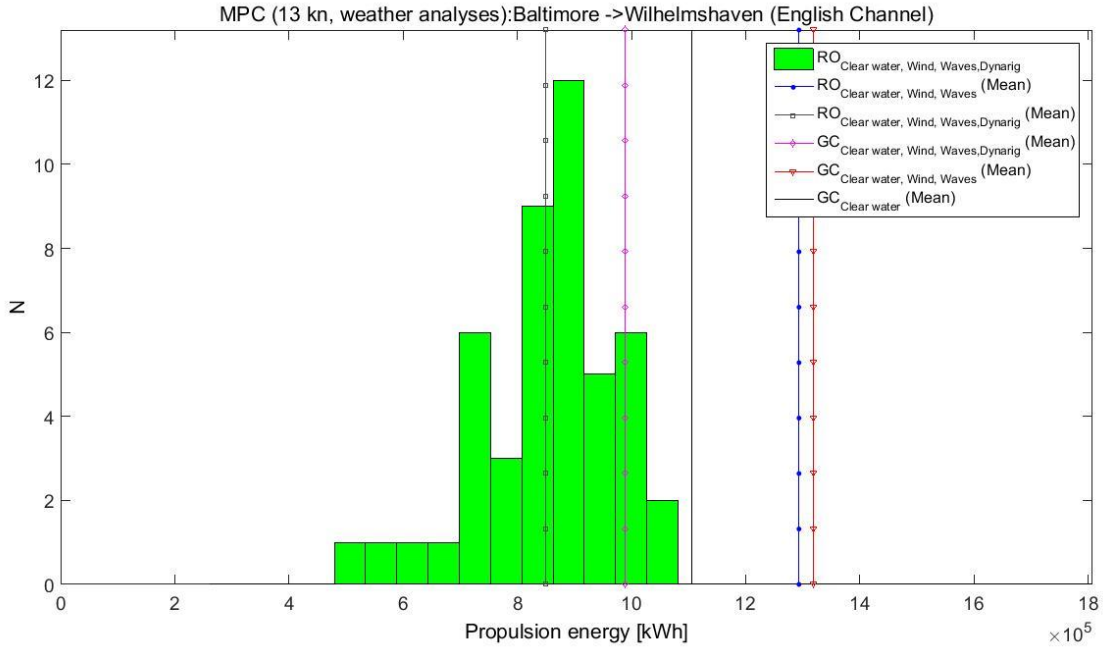

Figure 6: Energy consumption of a MPC sailing with 13 kn from Baltimore to Wilhelmshaven once a week in the year 2008. The perpendicular lines in the histogram represent long-term mean ship propulsion energy values for the respective settings that are shown in the legend. The mean values for the energy consumption are given for clear water resistance only, shown as well are the case with and without Dynarig and with route optimization (RO) and without route optimization (using the great circle route GC), but considering additional resistances by wind and waves. The histogram shows the distribution of energy values for a ship with a Dynarig considering clear water, wind and wave resistances; weather data = analysis data 2008

Table 1: Sea margin (in % of total energy consumption) for the 3 discussed routes, each route with RO and without RO (GC). Multipurpose carrier (MPC), 13 kn, mean values for one year (2008) with one journey / week; GC=great circle; RO = route optimization for minimum energy; > = from - to

Course / energy demand [%] of total energy	Sea margin on GC	Sea margin for RO	Saving by RO
Baltimore>Wilhelmshaven via Engl. Ch. Wilhelmshaven>Baltimore via Engl. Ch.	21 39	17 31	4 8
Nuevo Palmira>Emden Emden>Nuevo Palmira	20 13	18 12	2 1
Bergen>Wilhelmshaven Wilhelmshaven>Bergen	15 16	13 14	2 2

Table 2: Saving potential of the propulsion energy by different WPS in % (Flettner, Dynarig, Kite) on the route BA(Baltimore) –WHV(Wilhelmshaven) via English Channel, Vs=13kn, for a course on the GC and on an energy optimized course (RO)

Course /saving[%]	Flettner Rotor	Dynarig	Kite
BA>WHV; GC	21	25	23
BA>WHV; RO	31	35	29
WHV>BA; GC	14	21	10
WHV>BA; RO	24	33	19

Table 3: Saving potential with the Flettner Rotor on the 3 routes (in % to the sailing considering wind and waves, without WPS) for a MPC, Vs=13kn. compared for sailing on the GC of on the optimized route (RO).

Course / saving[%]	Flettner on GC	Flettner by RO
Baltimore>Wilhelmshaven via Pentland Wilhelmshaven>Baltimore via Pentland	24 15	35 27
Nuevo Palmira>Emden Emden>Nuevo Palmira	7 11	13 15
Bergen>Wilhelmshaven Wilhelmshaven>Bergen	15 16	20 19

(b) Energy saving by WPS on the North Atlantic route

In Table 2 the saving potentials (in % of the energy without WPS) for the 3 discussed WPS are compared on the North Atlantic route (for both directions), all WPS showing lower savings from east to west (upwind). The Dynarig gives the highest saving (up to 35%), especially on the route from east to west.

(c) Energy saving for different routes

In Table 3 the saving potential is shown for the three discussed routes when using a Flettner rotor. The North Atlantic route gives the highest saving of about 27– 35 %, when travelling on the optimized route. On the route to South America the weather is usually rather stable with moderate winds, yielding a saving potential of about 13% - 15%, rather independent from the shipping route direction. On the North Sea route (WHV-Bergen) the saving potential is about 20%, rather independent on the shipping route direction since the route travels perpendicular to the dominant wind direction (from west to east).

(d) Travel time

Figure 7 shows the travel time for the route Wilhelmshaven – Baltimore with and without RO. The increase in travel time due to the RO is in the order of about 5 hours as yearly mean value (maximum is 17 hours). Compared to the total travel time of 294 hours. it is about 2%. This is within the scope of the usual uncertainties of tramp shipping. It could be brought to zero, when adjusting the ship speed for a defined arrival time.

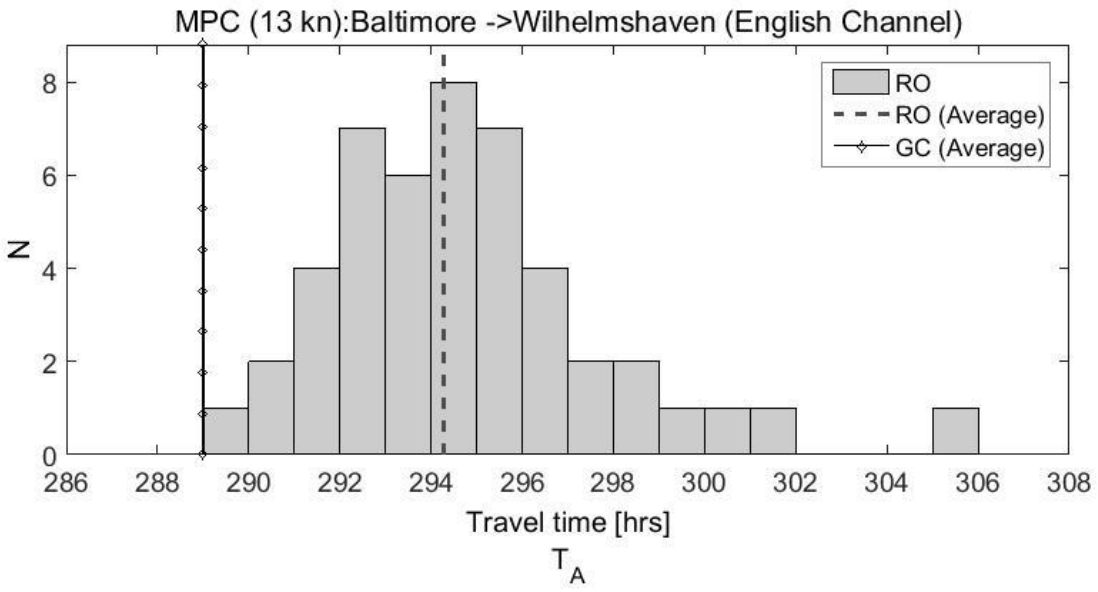

Figure 7: Distribution of the travelling time with the use of a WPS (here a Flettner rotor) with route optimization RO, compared to the travelling time on the great circle GC. Data obtained for sailing once a week from Baltimore to Wilhelmshaven; weather data = analysis data of 2008

6. UNCERTAINTY

The saving potential has been calculated by using the "actual weather data" (analysis data) along the route at the specific time. When planning an optimized route, it will be done on the basis of forecast data. A method to estimate the uncertainty of the energy saving with forecast data is developed as well (Zastrau, 2016).

7. ECONOMY

The realization of a WASP will mainly depend on the economy, but also on the impact of ship emissions on the environment (legal restrictions).

The actual cost-effectiveness mainly depends on

- The fuel price,
- the additional investment for a WPS,
- additional operating costs due to a WPS.
- The ship's speed

For a rough estimation of the investment for a WPS (without developing costs) it can be shown that a WPS on the discussed ships on windy routes such as the North Atlantic might be profitable for a fuel prices of the order of 500 € /to (profitability after 5 years) or 250 €/to (profitability after 10 years) (Schlaak, 2016). In these calculations, no costs due to the environmental impact are considered. Details will be discussed elsewhere.

8. CONCLUSION

The limited availability of oil in the future, connected with expected rises of fuel prices, and the impact of the emissions on the environment by nonrenewable energy, leads to the necessity to look for alternatives to the actual ship propulsion technology. There are several technologies under discussion as the use of LNG, or the use of wind assisted ship propulsion (WASP). Here the saving potential of WPS is calculated by simulating the energy consumption of selected ship types using a kite, or a Flettner rotor or a Dynarig sail as additional propulsion aid. The saving of energy by the different WPS are compared. It can be shown that on windy routes (as on the North Atlantic) a saving potential up to 35 % on optimized routes could be achieved with WPS which do not change the actual function of the discussed ships (speed, performance). With the price of the actual fuel used in seagoing ships a profitability is not yet given. However, considering the needed changes in the future due to the impact on environment and expected fuel prices developments, it can be deduced from this reported research that a development of WASP technologies might be reasonable.

9. ACKNOWLEGDEMENT

This research project was financed by the VW foundation, via the country of Lower Saxony, Germany.

10. REFERENCES

1. ALLENSTRÖM, B. (2012), *Wind propulsion - to be or not to be?* Highlights No. 56, SSPA Sweden AB, Göteborg, pp. 6–7.
2. BENTIN, M., ZASTRAU, D., SCHLAAK, M., FREYE, D., ELSNER, R. and KOTZUR, S. (2016), *A new Routing Optimization Tool. Influence of Wind and Waves on Fuel Consumption of Ships with and without Wind Assisted Ship Propulsion System*s, Proceedings of the 6th Transport Research Arena. April 2016, Warsaw, Poland.
3. BUNKER FUEL PRICES, *"Transport-related Price Indices"*, available at: http://www.transport.govt.nz/ourwork/tmif/transportpriceindices/ti008/ (Accessed 5th September 2016).
4. BUNKERINDEX (2016), available at: www.bunkerindex.com (Accessed 18th Sept. 2017)
5. DYKSTRA NAVAL ARCHITECTS (2013), *The Ecoliner Concept. Future Design in Progress*, through www.gdnp.nl (Accessed 10th September 2017).
6. ENERCON (2013), *Segelrotorschiff "E-Ship 1" spart im Betrieb bis zu 25 Prozent Treibstoff*, available at: http://www.enercon.de/p/downloads/PM_E-Ship1_Ergebnisse_DBU.pdf (Accessed 7th June 2015).
7. MALTESE FALCON (2016), available at: https://www.symaltesefalcon.com/index.php (Accessed 20th August 2017).
8. Otto, H. (1992), *Windantrieb für Schiffe*, Windenergie aktuell, Vol. No. 11 (1992)
9. PRÖLSS, W. (1970), *The economic possibilities of wind propelled cargo ships*. AYRS, UK
10. SCHENZLE, P. (2010), *Windschiffe im 21. Jahrhundert? Aktuelle Ansätze zum Windvortrieb von Schiffen*, Jahrbuch der Schiffbautechnischen Gesellschaft, 104 (2010), pp. 55–65.
11. SCHENZLE, P. (2016), *Warum Windschiffe oder Windzusatzantriebe: Beitrag auf der Abschlusskonferenz zum FSP ROBUST*, Wind of Change in Ocean Shipping, MARIKO, Leer, Germany.
12. SCHENZLE, P. AND HOLLENBACH, U. (2010), *Entwicklung der Segelschiffe Gestern und Heute: Windkraftnutzung auf See, Chancen für den Standort Hamburg*. HSVA - Kompetenzzentrum für Windschiffe, Hamburg, Germany
13. SCHLAAK, M. (2016), *Einsparpotenzial in der Seeschifffahrt*, Schiff & Hafen, Vol. 11 (Nov. 2016), pp. 40–45.
14. SCHLAAK, M., KREUTZER, R. AND ELSNER, R. (2009), *Simulating possible savings of the SkySails-system on international ship fleets*, Transactions of The Royal Institution of Naval Architects; Intl.J. Maritime Eng., No. 151, part A4, p. 25.
15. SEIFERT, J. (2012), *A review of the Magnus effect in aeronautics*, Progress in aerospace sciences: An international review journal, Vol. 55, Science Direct, Amsterdam, New York, pp. 17–45.
16. TRAUT, M., GILBERT, P., WALSH, C., BOWS, A., FILIPPONE, A., STANSBY, P. and WOOD, R. (2014), *Propulsive power contribution of a kite and a Flettner rotor on selected shipping routes*, Applied Energy, Vol. 113, pp. 362–372.
17. WAGNER, B. (1966), *Windkanalversuche mit gewölbten Plattensegeln mit Einzelmasten sowie mit Plattensegel bei Mehrmastanordnung*, TUHH, report 171, Hamburg, Germany.
18. WAGNER, C., ANDERSSON, G., RAULIEN, A., SAUER, I. and BELLON, M. (1985), *Weiterentwicklung des Flettner-Rotors zum modernen Windzusatzantrieb. Phase I, Band 1 + 2*, available at: https://www.tib.eu:Weiterentwicklung des Flettner-Rotors zum modernen Windzusatzantrieb, Blohm & Voss AG, Hamburg, TIBKAT, 1985, (Accessed 10th September 2017)
19. www.decaboyachtpainting.com, *Project Maltese Falcon*, available at: ttp://www.decaboyachtpainting.com/?project=maltese-falcon&lang=de (Accessed 10th 2016).
20. ZASTRAU, D. (2016), *Estimation of Uncertainty of Weather-dependent Energy Predictions with Application to Weather Routing and Wind Power Generation*, Dissertation, tzi, University Bremen, Bremen, 2016.